Accepted Manuscript

Transfection Efficiency and Transgene Expression Kinetics of mRNA Delivered in Naked and Nanoparticle Format

Kyle K.L. Phua, Kam W.Leong, Smita K. Nair

Please cite this article as: Kyle K.L. Phua, Kam W.Leong, Smita K. Nair, Transfection Efficiency and Transgene Expression Kinetics of mRNA Delivered in Naked and Nanoparticle Format, *Journal of Controlled Release* (2013), doi: 10.1016/j.jconrel.2012.12.029

Transfection Efficiency and Transgene Expression Kinetics of mRNA Delivered in Naked and Nanoparticle Format

Kyle K.L Phua[1], Kam W.Leong[1*,2], Smita K. Nair[2]

[1]Department of Biomedical Engineering, Duke University, Durham, North Carolina, 27708, USA
[2]Department of Surgery, Duke University Medical Center, Durham, North Carolina, 27710, USA

* To whom correspondence should be addressed: Department of Biomedical Engineering, Duke University, Box 90281, Durham, NC 27708, USA. Tel.: +1 919 660 8466.
E-mail address: kam.leong@duke.edu.

Abstract

Transfection efficiencies and transgene expression kinetics of messenger RNA (mRNA), an emerging class of nucleic acid-based therapeutics, have been poorly characterized. In this study, we evaluated transfection efficiencies of mRNA delivered in naked and nanoparticle format *in vitro* and *in vivo* using GFP and luciferase as reporters. While mRNA nanoparticles transfect primary human and mouse dendritic cells (DCs) efficiently *in vitro*, naked mRNA could not produce any detectable gene product. Protein expression of nanoparticle-mediated transfection *in vitro* peaks rapidly within 5-7 hours and decays in a biphasic manner. *In vivo*, naked mRNA is more efficient than mRNA nanoparticles when administered subcutaneously. In contrast, mRNA nanoparticle performs better when administered intranasally and intravenously. Gene expression is most transient when delivered intravenously in nanoparticle format with an apparent half-life of 1.4 hours and lasts less than 24 hours, and most sustained when delivered in the naked format subcutaneously at the base of tail with an apparent half-life of 18 hours and persists for at least 6 days. Notably, exponential decreases in protein expression are consistently observed post-delivery of mRNA *in vivo* regardless of the mode of delivery (naked or nanoparticle) or the site of administration. This study elucidates the performance of mRNA transfection and suggests a niche for mRNA therapeutics when predictable *in vivo* transgene expression kinetics is imperative.

Graphical Abstract:
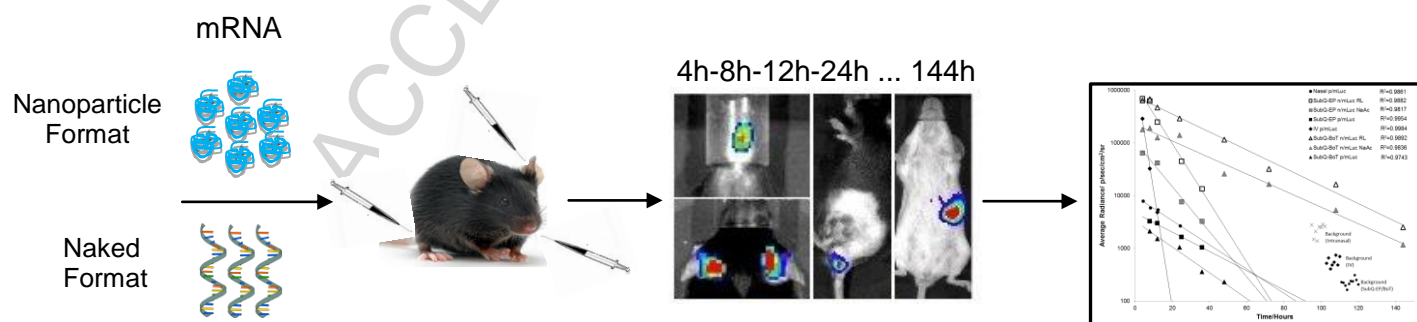
Introduction

The development of mRNA therapeutics received a significant boost following studies that demonstrated dendritic cells (DCs) pulsed with mRNA *in vitro* could become potent antigen-presenting cells *in vivo*[1]. Various delivery methods were explored to ascertain the most efficient method to transfect DCs with mRNA [2] and electroporation emerged as the preferred method. *Ex vivo* approaches to vaccination using autologous blood-derived DCs electroporated with tumor mRNA were developed and translated into clinical studies in patients with cancer [3]. Nevertheless, nanoparticle-mediated delivery of mRNA to DCs warrants attention because of its potential advantages, the most important of which is the possibility of direct *in vivo* administration of mRNA vaccines without *ex vivo* manipulation of DCs. Encapsulation of mRNA in nanoparticles can also protect the mRNA from nuclease degradation, facilitate uptake, promote endosome escape, and provide conjugation sites to attach DC-specific receptor ligands for targeted delivery. An alternative that has been extensively investigated is *in vivo* administration of naked mRNA, which has been shown feasible to engender immune responses. Structural modifications such as length of poly-A tail [4], modified cap analogues [5], and pseudouridine substitution [6] as well as the use of Ringer's Lactate (RL) [7] have enhanced naked mRNA transfection efficiency *in vivo*.

As a rapidly emerging class of nucleic acid therapeutics, there are key benefits in using mRNA over plasmid DNA for vaccine or therapeutic applications. First, mRNA contains no viral promoters (e.g. CMV) and bacterial sequences that can cause toxicity. Second, mRNA does not integrate into host genome, which may lead to deleterious mutation [8]. Third, gene expression via mRNA is relatively transient and therefore safer to use compared to DNA. Last but not least, as mRNA does not need to cross the nuclear envelop, it increase the chances of successfully transfecting quiescent cells such as DCs. Indeed, mRNA can mediate a higher level of protein expression *in vivo* compared to DNA over shorter durations [7]. Most recently, encouraging *in vivo* transfection mediated by naked mRNA has been reported where calcium-containing buffers such as Hank's Balanced Salt Solution or Ringer's Lactate are used in the injection [9].

mRNA delivery to DCs using nanoparticles has also been recently explored. Su et al [10] adsorbed GFP-encoding mRNA to a pegylated and lipid-coated cationic core to obtain a 30% transfection efficiency on DC2.4 cells *in vitro,* and achieved *in vivo* gene expression via intranasal administration. Perche et al [11] encapsulated GFP mRNA into mannosylated lipopolyplexes and achieved approximately 60% transfection efficiency on DC2.4 cells *in vitro*. They also observed anti-tumor effects when mice were vaccinated intravenously with lipopolyplexes encapsulating the antigen mRNA. Intuitively, mRNA encapsulated in nanoparticles should mediate higher transfection efficiencies *in vivo*, but given the encouraging data reported on naked mRNA transfections, it becomes necessary to evaluate and compare transfection efficiency of gene carrier-mediated mRNA with naked mRNA delivery *in vivo*. In this paper, we hypothesize that mRNA delivered in nanoparticle format can be, in some ways, more efficient than naked mRNA. Using a commercially available mRNA transfection reagent, we show that it is possible to formulate stable mRNA nanoparticles in small volumes compatible with *in vivo* administration. We then evaluate and compare transfection efficiencies and transgene expression kinetics of these mRNA formulations (p/mRNA) with naked mRNA (n/mRNA) on primary human and mouse DCs *in vitro*. This comparative evaluation is then

performed *in vivo* at four potential vaccination sites: subcutaneous (ear pinnae 'SubQ-EP' and base of tail 'SubQ-BOT'), intranasal and intravenous.

Materials and Methods

Ethics Statement

Human: Primary human cells used in these experiments were isolated from blood obtained from healthy human volunteers following informed written consent using a protocol approved by the Duke University Institutional Review Board.

Murine: In conducting the research described in this paper, the investigators adhered to the "Guide for the Care and Use of Laboratory Animals" as proposed by the committee on care of Laboratory Animal Resources Commission on Life Sciences, National Research Council. The facilities at the Duke vivarium are fully accredited by the American Association for Accreditation of Laboratory Animal Care (AAALAC), and all studies were conducted using a protocol approved by the Duke University IACUC.

Cell Lines and Mice

Jaws II cells were obtained from ATCC and DC2.4 cells was a kind gift from Dr. Kenneth Rock. 5-6 weeks old C57BL/6 or Balb/c mice from Jackson Lab were used for transfection experiments. Balb/c mice were used for intravenous (IV) administrations while C57BL/6 mice were used all other routes of injection. Human DCs and murine DCs were derived using previously reported protocols [12] from adherent monocyte obtained peripheral blood mononuclear cells (PBMCs) and bone marrow precursor cells from C57Bl/6 mice, respectively.

In vitro Transcription, Nanoparticle Formulation and Characterization.

In vitro Transcription (IVT) kit and ARCA cap were purchased from New England Biolabs and Trilink Biotech respectively. Luciferin was obtained from Biosynth International. IVT was performed according to manufacturer's protocol. An initial GTP/ARCA cap ratio of 1:3 was used and slightly adjusted to ensure mRNA yield was 40-50 μg/reaction. Adjustment is necessary to ensure a consistent capping efficiency of ~80%. Stemfect mRNA transfection reagent was purchased from Stemgent. RNAse free sodium acetate (Ambion) was adjusted with hydrochloric acid to pH 5 and subsequently diluted with RNAse-free glucose to 100 mM/5% glucose (NaAc buffer). mRNA nanoparticles were formulated by adding 8 μl ethanolic reagent to 10 μl of mRNA (0.2 μg/μl) suspended in NaAc buffer under gentle vortexing. Vortex speed was optimized to prevent mRNA degradation from excessive shear stress. The mixture was adjusted to appropriate volumes/pH and incubated at room temperature (RT) under vacuum to completely remove ethanol. Size and zeta potential measurements were obtained using the NanoZS (Malvern) by diluting the 10 μl nanoparticles (0.2 μg/μl) into 100 μl of DI water or mouse serum (diluted with sterile water to obtain respective concentrations). Mouse serum was obtained from whole blood of C57BL/6 mice. Whole blood was obtained by cardiac puncture and allowed to clot for 10 min at room temperature. Cells were removed via centrifugation (4000rpm) at 4°C. Supernatant (without buffy coat) was removed and centrifuged again at 4°C to completely remove suspended particles.

In vitro Transfection and Kinetics

For analysis of GFP expression, cell lines were seeded at a density of 8×10^4 cells/well while primary DCs were seeded at a density of 1.5×10^5 cells/well on 24-well plates. Cells were transfected with nanoparticles at 0.5 µg/well (cell lines) and 1.3 µg/well (primary cells). Transfections were done in the presence of serum. For human DCs, heat inactivated FBS was added to AIM V media to a final concentration of 10%. GFP expression was assayed by flow cytometry 8 hours post-coculture of cells with mRNA.

For analysis of luciferase expression, cells were seeded at a density of 3×10^4 cells/well on 96-well white opaque plates (Nunc). Cells were transfected with nanoparticles at 0.4 µg/well and analyzed at various time points. Before assay, microplates were centrifuged (1000 rpm, 5 min), media aspirated and cells were lysed with 75 µl Glo-Lysis buffer. Luciferase expression was assayed by adding an equal volume of Steady-Glo Luciferase substrate (Promega). Bioluminescence was measured by plate reader (Optima) with 15-second exposure time for human DCs and a 10-second exposure time for mouse DCs.

In vivo Transfection and Kinetics

Nanoparticles were prepared at 0.2 µg/µl as described above, combined and adjusted with 5% glucose to appropriate volumes. Naked mRNA controls were diluted in NaAc buffer (5% glucose/100 mM NaAc, pH5) and Ringer's Lactate (Baxter) respectively. Where indicated, 1M Hepes was added to adjust the pH to 7.4 (monitored using pH paper). Anesthesia was achieved using isofluorane, if required.

Subcutaneous injection: Mice were injected with 4 µg mLuc in 40 µl subcutaneously at the base of each ear pinnae under anesthesia or with 8 µg mLuc in 60 µl at the base of tail. RNAse inhibitor (New England Biolabs), where applicable, is added to a final concentration of 1unit/µl. Intranasal injection: 4 µg in 20 µl was gently pipetted into the nostrils of anesthetized mice. Intravenous injection: 26 µg of mLuc nanoparticles in 200 µl was injected intravenously via tail vein.

A new syringe was used for each injection. There was no incidence where 2 or more doses were drawn into the same syringe and injected sequentially into 2 or more mice. Luciferase expression was monitored non-invasively at 4, 8, 12, 24 and 36-144 hours (SubQ only) post-injection with IVIS Caliper 100 Imaging System. Each mouse was administered with 200 µl of luciferin (28.5 mg/ml dissolved in PBS) intraperitoneally at all indicated time points. To prevent false positive readings, non-transfected controls were always included on the same platform and imaged at the same time.

Statistics

Statistical analysis was performed using correlation functions for two-tailed Student's t-Test or One-way Anova (followed by Bonferroni Multiple Comparison Test) with the software Graph Pad Prism.

Regression Analysis

Transgene expression kinetics data were fitted into a first order exponential decay model:

$y=A*exp(-\lambda t)$, where y = bioluminescence in photons/sec/cm^2/sr, t = time in hours, A is the bioluminescence at t=0 and λ is the decay constant. Apparent half-lives were derived using the formula $t_{1/2}= \ln(2)/\lambda$.

Results
Primary DCs can be efficiently transfected with mRNA nanoparticles.
mRNA nanoparticles formulated with Stemfect mRNA transfection reagent, even when formulated at a concentration as high as 0.2 µg/µl, were colloidally stable in NaAc buffer with an average diameter of 150 nm (PDI=0.2). They aggregated gradually in various dilutions of mouse serum but remained stable for at least 80 min with an average diameter below 350 nm, a size that remained conducive for endocytosis (Fig.1A). GFP mRNA nanoparticles were highly efficient *in vitro*. DC2.4 cells were transfected with a transfection efficiency >97%. JAWS II cells, which were morphologically more consistent with primary mouse DCs, were transfected reproducibly with at least 80% GFP+ efficiency. The transfection efficiencies of primary mouse and human DCs were >60% and >50% respectively (Fig.1B). These transfection efficiencies, to the best of our knowledge, were the highest in literature for mRNA nanoparticle delivery to DCs *in vitro*. Naked mRNA, however, failed to transfect any of the DC lines (Fig. 1B).
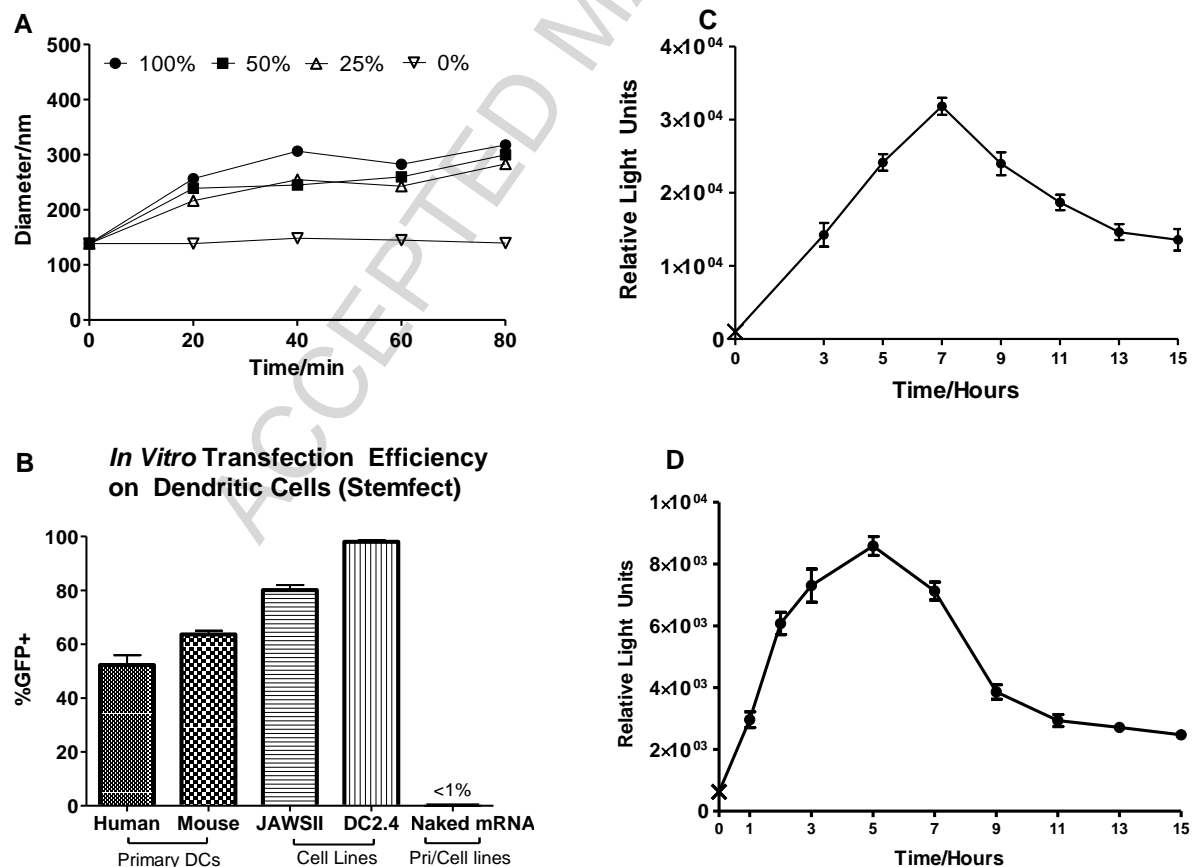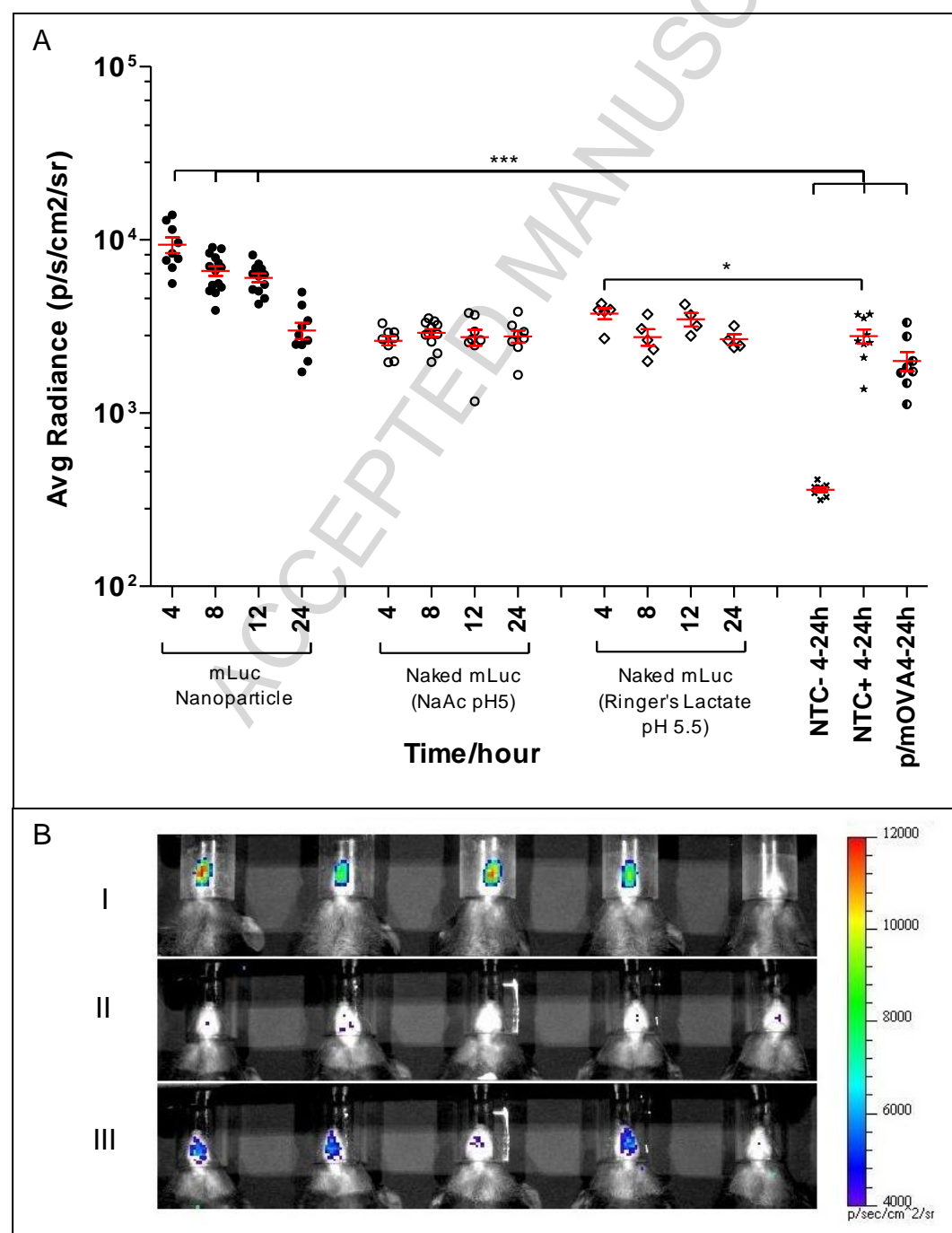

Fig. 1. Evaluating transfection efficiency of nanoparticle mRNA and naked mRNA *in vitro*. (A) Aggregation kinetics of p/mLuc in 0-100% mouse serum. (B) *In vitro* p/mGFP and n/mGFP transfection of primary DCs and DC cell lines. (C), (D) *In vitro* p/mLuc transgene expression kinetics of primary human peripheral blood monocyte-derived DCs and primary mouse bone marrow precursor-derived DCs respectively ('X' represents background luminescence). Cells seeded on the same 96-well plate were transfected at various time points with 0.4 µg mLuc (n=5) and assayed after 15 hours. Results were averages of 3 independent experiments.

In vitro transgene expression kinetics on DC cell lines with mRNA nanoparticles were consistent with other cell types reported in literature [13]. We also observed similar kinetics in primary mouse and human DCs (Fig.1C and D). Mouse DCs expressed luciferase within the first hour of transfection, much earlier than the typical 2-4 hour incubation time used for *in vitro* transfection. Transgene expression peaked rapidly at 5-hour post-transfection and interestingly tapered off in a bi-phasic manner: a rapid and almost symmetrical drop in expression at the 9-hour time-point followed by a more gradual decrease that extended beyond 15-hr post-transfection. The trend in primary human DCs was similar although expression rose more gradually to peak at 7-hour post-transfection.
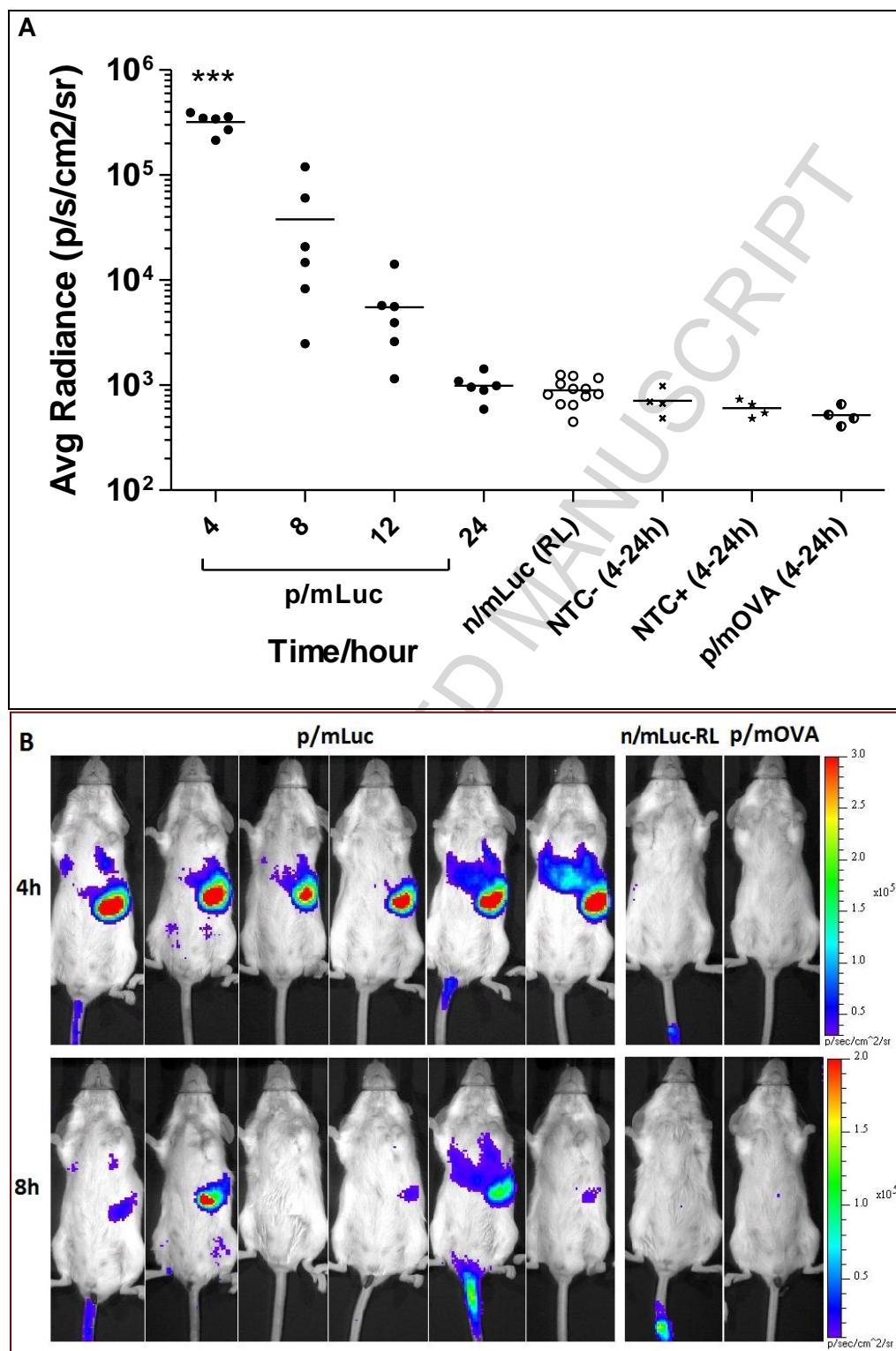
Fig. 2. Evaluating in vivo transfection efficiency of nanoparticle mRNA and naked mRNA administered intranasally. (A) Bioluminescence in C57BL/6 mice transfected intranasally with 4 µg of p/mLuc and n/mLuc over a 24 hour time period. NTC-: Non Transfected Control, no luciferin injected; NTC+: Non Transfected Control, luciferin injected; p/mOVA: mOVA nanoparticle (B) Representative set of IVIS images of nasally transfected mice 4 h post-intranasal delivery: (i) p/mLuc (ii) n/mLuc in NaAc Buffer (iii) n/mLuc in Ringer's Lactate. Fifth mouse in panels (i) to (iii) is NTC+. *** p<0.0001 compared to p/mOVA, NTC- and NTC+ based on one-way anova (all 15 groups) followed by bonferroni multiple comparison test. * p<0.05 based on two tailed student's t-test.

## Nasal cavity can be consistently transfected with p/mRNA but not n/mRNA.

When administered intranasally, only mLuc delivered in nanoparticle form (p/mLuc) resulted in consistent and statistically significant bioluminescence (Fig.2A) over negative controls (non-transfected mice and mice transfected with mOVA nanoparticle). Luciferase expression peaked at about 4 hours and decayed exponentially to near background at 24 hours post-mRNA delivery. Expression levels mediated by p/mLuc were consistently detected in 5 independent experiments (n>15) and were not confounded by false positives. Bioluminescence signal with mLuc delivered in naked form (n/mLuc) were similar to negative controls. However, we were able to observe weak signals (but statistically significant (p <0.05) bioluminescence in mice transfected with n/mLuc-RL. This signal was only evident at 4-hour post-mRNA delivery (Fig. 2). It should be noted that negative controls when injected with luciferin also showed detectable bioluminescence at the nasal site (creating false positives) as shown in Fig. 2A.

Luciferase expression of nanoparticle mRNA in the RES is short lived after intravenous administration

As shown in Fig. 3A, the only time we could detect any bioluminescence using the intravenous mode of delivery was following p/mLuc administration. Bioluminescence following n/mLuc delivery was observed only around the site of injection in the tail skin, presumably caused by leakage into the subcutaneous space during IV injection (Fig. 3B). As expected, serum nucleases were efficient in degrading naked mRNA even when dissolved in Ringer's Lactate, reinforcing the notion that any enhancement mediated by Ringer's Lactate was not due to mRNA protection. Interestingly, transfection was observed predominantly at the spleen instead of liver and may be attributed to gene carrier property. However, the luciferase expression was short lived. While expression could be detected in some mice at other sites after 24 hours, splenic luciferase expression was undetectable after 24 hours in all mice. Tissue barriers (super fascia, skin and fur) might have scattered weaker signals that would otherwise be detected. In some mice, injected particles leaked into the subcutaneous space transfecting skin of tail (Fig. 3B, mouse #1 and #5). This provided a convenient internal control that further confirmed rapid clearance of luciferase from the spleen. As initial luciferase expression levels were reasonably high (average radiance between 10^5- 10^6), its short-lived kinetics might not be attributed to poor transfection but likely indicated rapid breakdown of luciferase protein and/or mRNA in splenic cells.

Fig. 3. Evaluating in vivo transfection efficiency of nanoparticle mRNA and naked mRNA administered intravenously. (A) Bioluminescence signal in BALB/c mice intravenously administered with 26 μg of p/mLuc and m/Luc. (B) IVIS images of mice transfected in (A) at 4 and 8 h time points with respective color scales. p/mOVA: mOVA nanoparticle NTC-: Non Transfected Control, luciferin not injected; NTC+: Non Transfected Control, luciferin injected. *** p<0.0001 compared to n/mLuc, p/mOVA, NTC- and NTC+ based one-way anova (all 8 groups) followed by bonferroni multiple comparison test.
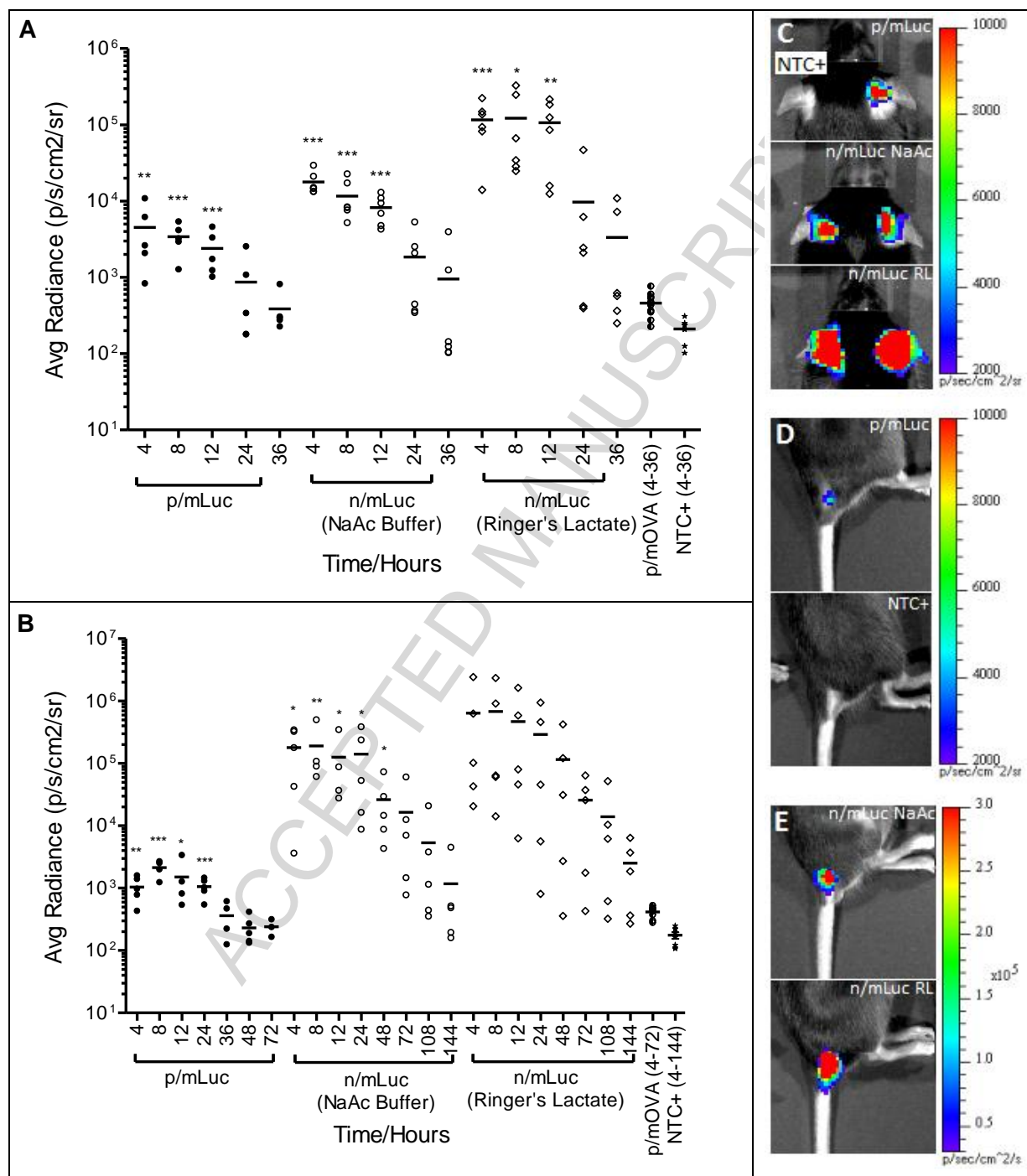
Fig. 4. Evaluation of in vivo bioluminescence after subcutaneous injection of mRNA
(A) *In vivo* bioluminescence in C57BL/6 mice transfected subcutaneously at the base of the ear pinna (SubQ-EP) with p/mLuc and n/Luc (in NaAc and RL) from 4-36 hours. **(B)** *In vivo* bioluminescence in C57BL/6 mice transfected subcutaneously at the base of tail (SubQ-BOT) with p/mLuc and n/Luc (in NaAc and RL) from 4-144 hours. pH of p/mLuc and NaAc buffer was adjusted to 7.4 with 1M Hepes, while pH of Ringer's Lactate was kept at its native value of 5.5. **(C, D, E)** Representative IVIS images of transfected mice ear-pinnae **(C)** and base of tail **(D)** and **(E)** base of tail 4h post injection. *, **, ***: p<0.05, 0.005, 0.001 respectively based on two-tailed Student's t-test (p/mLuc vs p/mOVA, n/mLuc vs NTC+). Detailed statistical analysis of **(A)** reported in Supplementary Fig. S2.

Naked mRNA mediates higher and more sustained transfection than nanoparticle mRNA when delivered subcutaneously.

When we compared naked versus the nanoparticle format for mRNA delivery at subcutaneous sites, n/mRNA was significantly more efficient than p/mRNA with higher transfection efficiencies. As shown in Fig. 4A, both p/mLuc and n/mLuc were capable of transfecting subcutaneous tissue at ear pinnae with statistically significant levels for at least 12 hours. In particular, when n/mLuc was dissolved in Ringer's Lactate, luciferase expression was more than one order of magnitude above p/mLuc at the ear-pinnae site. This was unexpected because we previously showed that p/mRNA possessed good colloidal stability (Fig. 1) and has been shown by the manufacturer to transfect primary fibroblasts efficiently. The contrast between both delivery formats was more striking at the base-of-tail subcutaneous site (Fig. 4B). This particular site was chosen because of enhanced lymphatic drainage to the inguinal lymph node in mice. At SubQ base-of-tail site, statistically significant levels of luciferase could be detected in all groups for at least 24 hours. It should be noted that a higher mLuc dose (8 μg) was applied because we could not detect consistent luciferase expression with 4 μg of mRNA. Interestingly, expression at base-of-tail lasted for more than 6 days, with luciferase expression still detectable in 3 out of 5 n/mLuc-RL transfected mice at the end of day 6. Within the n/mLuc groups, greater transfection enhancement by Ringer's Lactate was observed at ear pinnae site compared to base-of-tail site of injection. Overall, gene expression by n/mLuc at both SubQ sites was sustained and at 1-2.5 orders of magnitude higher compared to p/mLuc.

Subcutaneous (SubQ) Transfection is pH dependent, but independent of RNAse inhibitor.

When n/mLuc was injected SubQ-EP, we observed as others did, an enhancement in naked mRNA transfection with calcium-containing Ringer's Lactate. As shown in Fig. 5A, the transfection efficiency of naked mRNA was not further enhanced, nor deteriorated when injected together with RNase inhibitor. Hence, RNAse did not appear to pose a problem to n/mRNA at SubQ sites. In addition, as RNase inhibitor used was a protein, our data further suggested that the addition of proteins in mRNA did not affect n/mRNA transfection. We also observed that acidic pH reduced transfection efficiency of n/mRNA (Fig.5B). When neutralized with Hepes, statistically significant enhancement in transfection was observed. As the native pH of Ringer's lactate was 5.5, we investigated whether physiological pH might further increase the transfection efficiency. However, we did not detect any enhancement in transfection efficiency (Fig. 5B), indicating that the use of Ringers' Lactate rendered transfection insensitive to pH.
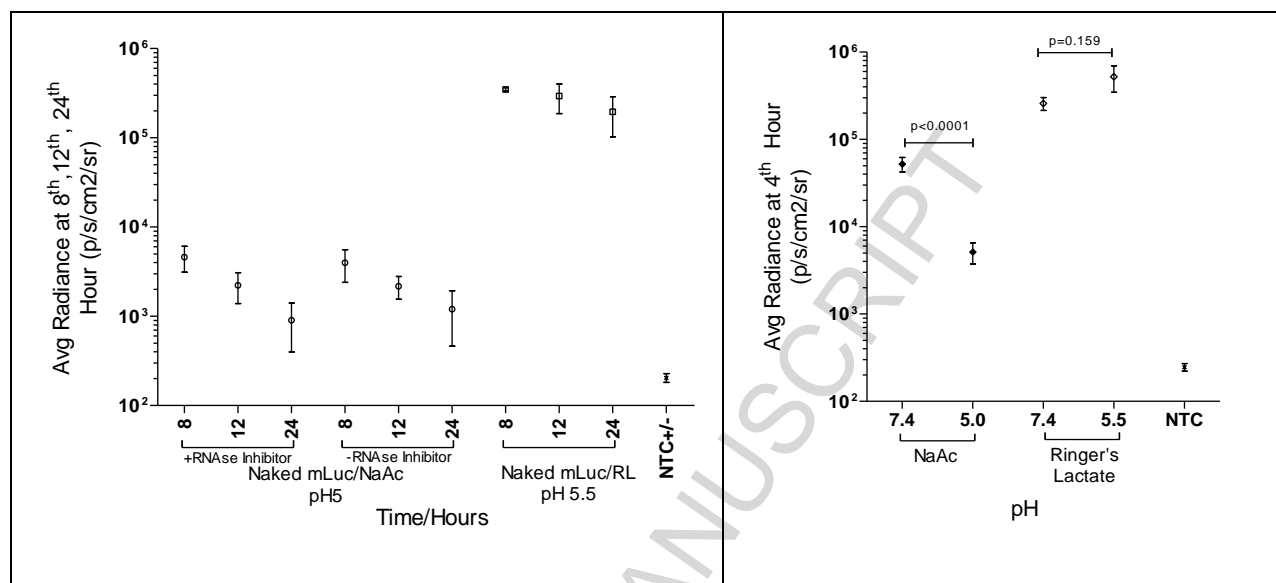
Fig. 5. (A) Effect of RNAse inhibitor on n/mLuc transfection at SubQ-EP. C57BL/6 mice were transfected with n/Luc +/-RNAse inhibitor (1unit/µl) at SubQ-EP. Bioluminescence was assayed at 8, 12, and 24 h. (B) Effect of pH on n/mLuc transfection. C57BL/6 mice were transfected with n/Luc dissolved in NaAc (pH 5 or 7.4) and Ringer's Lactate (pH 5.5 or 7.4). pH was adjusted with 1M Hepes. Bioluminescence was assayed at 4 h post injection. p value was calculated using two-tailed student's t-test.

Exponential decrease of transgene level with time at all sites of administration.

The luciferase expression kinetics were characterized by an exponential decrease in gene expression that could be fitted into exponential curves based on first order decay kinetics $y=Ae^{-\lambda t}$ (Fig. 6 and Supplementary Fig. S1). The trend was unexpectedly consistent and did not depend on the site of injection ($R^2 = 0.97$-0.99) or delivery format. Hence, *apparent* half-lives of luciferase protein expressed by mLuc *in vivo* could be computed and were tabulated in Table 1. Apparent luciferase half-lives determined for p/mLuc were relatively consistent across all sites (except IV). While the trend was consistent at subcutaneous sites, apparent half-lives of n/mLuc at SubQ-BOT were higher compared to SubQ-EP. We also observed an inverse relationship between transfection efficiency and apparent half-lives in the n/mLuc group. The use of Ringer's Lactate in n/mLuc transfections increased the transfection efficiencies, but also slightly decreased apparent half-lives at both base-of-tail and ear-pinna sites.
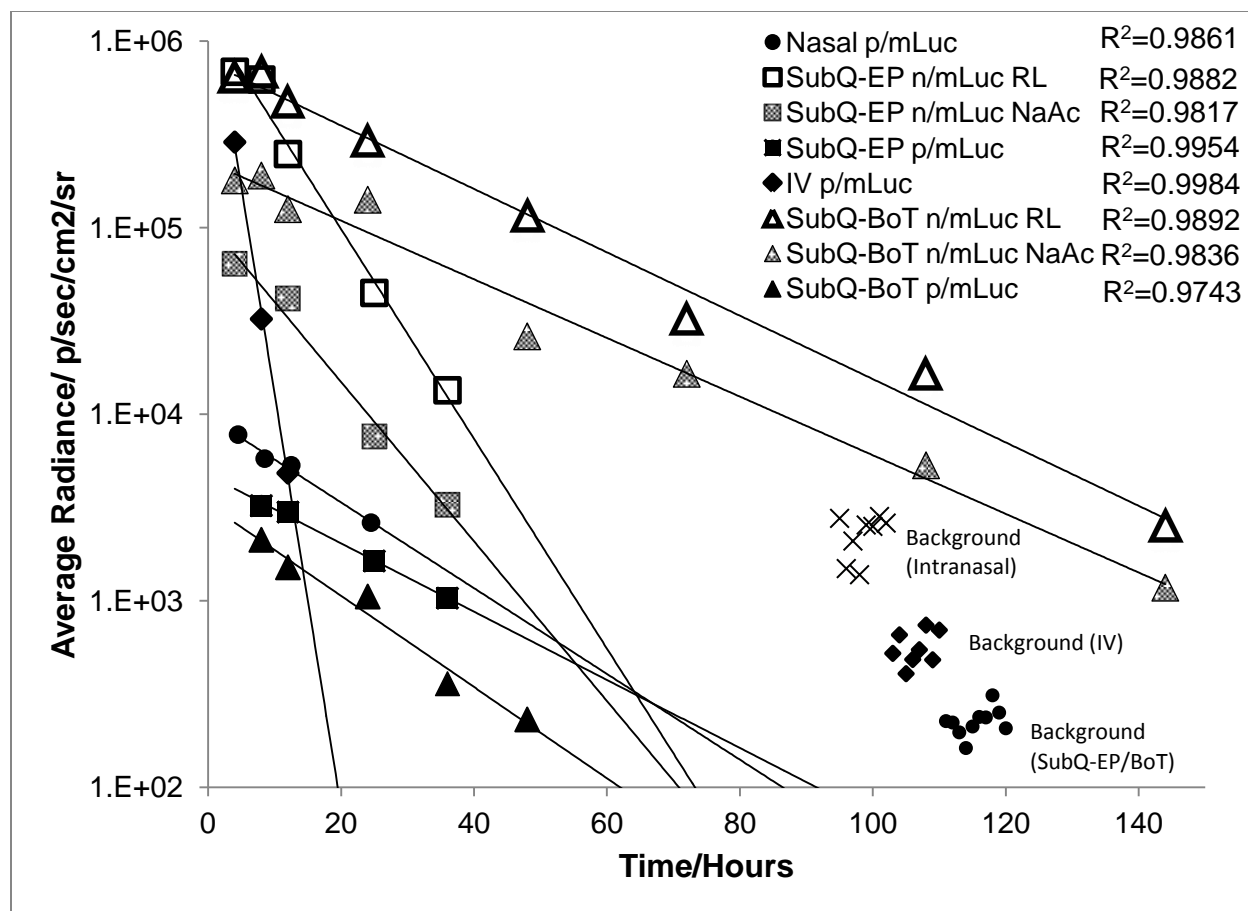
Fig. 6. Regression analysis of luciferase expression kinetics in vivo. Representative curves from each site/format were shown above. Additional regression curves were shown in Supplementary Fig. S2.

Table 1. Apparent *in vivo* half-life of luciferase protein expressed from mRNA

Apparent Luciferase Half-Lives Expressed From mRNA			
Administration Site	Delivery Format/Buffer	Decay Constant λ	Apparent Half-life/h
Intranasal	p/mLuc Exp 1	0.044	15.8
Intranasal	p/mLuc Exp 2	0.054	12.8
Intranasal	p/mLuc Exp 3	0.053	13.1
SubQ-Base of tail	p/mLuc NaAc	0.056	12.4
SubQ-Ear Pinnae	p/mLuc NaAc Exp 1	0.051	13.6
SubQ-Ear Pinnae	p/mLuc NaAc Exp 2	0.042	16.5
Intravenous	p/mLuc NaAc	0.510	1.4
SubQ-Base of tail	n/mLuc NaAc	0.036	19.3
SubQ-Base of tail	n/mLuc RL	0.039	17.8
SubQ-Ear Pinnae	n/mLuc NaAc Exp 1	0.098	7.1
SubQ-Ear Pinnae	n/mLuc NaAc Exp 2	0.092	7.5
SubQ-Ear Pinnae	n/mLuc RL Exp 1	0.129	5.4
SubQ-Ear Pinnae	n/mLuc RL Exp 2	0.138	5.0

Discussion:

Reports on nanoparticle-mediated delivery of mRNA, particularly in vivo, are relatively scarce compared to DNA delivery despite the advantages of obviating nuclear entry, avoiding insertional mutagenesis and more rapid gene expression. The transient and non-integrating nature of mRNA transfection is well suited for genetic vaccination. In this study, we first evaluated a number of mRNA nanoparticle formulations against dendritic cells with respect to their transfection efficiency, cytotoxicity, and colloidal stability at high concentration. The last parameter is important because it will allow us to vaccinate at a high dose in small injection volume. Of all gene carriers screened (Supplementary Fig. S3), which include lipofectamine, chitosan, PEI (25kda), polyamidoamine (CBA-ABOL) [14] and lipopolyplexes of DOTAP/Chol and DOTAP/DOPE/Chol, Stemfect® produced the best results. In DC2.4 cell line, Stemfect attained a transfection efficiency of 97% (GFP+ population) compared to 60% by Perche et al [11], 30% by Su et al[10] and 50% by Cheng et al [15]. There has not been any report on mRNA nanoparticle transfection of primary DCs, and we find that mRNA nanoparticles formulated using Stemfect transfect primary human and mouse DCs at transfection efficiencies of 52% and 64% (GFP+ cells) respectively. Our study provides encouraging direct evidence to proof the concept that it is possible to transfect primary DCs efficiently using mRNA nanoparticles. With the exception of one study reported by Perche et al [11], mRNA vaccination has relied on the application of naked mRNA. In this study, we systematically compare the performance of mRNA nanoparticles formulated using Stemfect (p/mLuc) versus naked mRNA (n/mLuc) in intranasal, intravenous, or subcutaneous administrations. While p/mLuc outperforms n/mLuc in both intranasal and intravenous delivery, n/mLuc produces higher and more sustained transgene expression in subcutaneous injection. Since the intranasal and intravenous routes target directly the Nasal Associated Lymphoid Tissues (NALT) and the spleen respectively, this study indicates the utility of nanoparticle-mediated mRNA for vaccination.

Aside from targeting NALT, nasal administration of vaccine is popular due to its non-invasive nature. We show that p/mLuc (4μg dose) consistently achieves gene expression in the nasal cavity with an average radiance of 9×10^3 p/sec/cm2/sr at 4-hr post-delivery, whereas n/mLuc only produces background level at all time-points. Compared to the only other study that reported intranasal mRNA nanoparticle transfection (4μg dose) [10] , this is the highest *in vivo* transfection efficiency we have observed. Within the n/mLuc groups, we are only able to detect bioluminescence from n/Luc (RL group) at 4th hour time point. Despite being transient, our finding highlights a significant contrast with naked pDNA, which does not transfect the nasal mucosa[16]. As the residence time of n/mLuc and p/mLuc in the nasal cavity is similar (Supplementary Fig. S4), higher transfection efficiency of p/mLuc is unlikely due to better mucoadhesion. Furthermore, since RL is known to improve naked mRNA transfections via enhanced cellular uptake [7], we can reasonably infer that n/mLuc transfects poorly due to RNAse present in the nasal tissues. In our study, we also consistently detect bioluminescence from nasal cavities of non-transfected mice that are injected with luciferin (NTC+, Fig. 2A) compared to those without luciferin (NTC-, Fig. 2A). The difference, in photons/sec/cm^2/sr, between NTC+ and NTC- is about one order of magnitude (Fig 2A). This appears to be unique to intranasal site as no such differences are observed in the spleen, ear pinna and base-of-tail.

In contrast with other transfected sites, luciferase expression is most short-lived when delivered via intravenous route, which coincidentally targets the spleen. The near spleen-specific transfection is likely due to the unique properties of the gene carrier, which is closely related to a

class of lipidoid previous reported for siRNA delivery [17]. We also speculate that the colloidal stability of the nanoparticles in mouse serum promotes biodistribution to the spleen. In a preliminary experiment where we formulated p/mLuc with an un-optimized protocol that led to aggregation, transfection in the liver is also observed (Supplementary Fig.5). In Fig.3, where p/mLuc are formulated with an optimized protocol, moderate levels of transfection in the liver can still be observed in 2/6 mice. Bulk mixing, the method used to formulate p/mLuc nanoparticles for this study, produces mRNA nanoparticles that are heterogeneous in size, surface charge, and likely composition. Recent literature has shown that a more controlled self-assembly of lipoplexes and polyplexes may lead to better performance with respect to colloidal stability, transfection efficiency, and even cytotoxicity[18-20]. These observations suggest that a more controlled formulation of the mRNA nanoparticles may improve and better predict in vivo performance.

The significantly shorter half-life of luciferase at the spleen may be attributed to transfection of antigen presenting cells, which are very efficient in breaking down endogenous protein and presenting them on MHC complexes. In our hands, intravenously administered p/mRNA has an apparent half-life of 1.4 hours (R^2=0.9984, N=6) and becomes undetectable at 24 hours. Unlike the subcutaneous or intranasal sites, the spleen is found under several layers of tissues and would have a higher threshold of detection, which may have contributed to a shorter apparent half-life as weaker luminescence at later time-points may not be detected.

Subcutaneous transfection with naked mRNA is well studied, but direct comparison with mRNA polyplexes or lipoplexes has not been reported. In this study, we reproduced published data where n/mLuc transfection is enhanced by RL at SubQ-EP by an order of magnitude [7]. We also observe n/mLuc outperforming p/mLuc, not unlike pDNA transfection where naked DNA is often superior, if not equal, to polyplexes in intramuscular or subcutaneous transfection [21, 22]. Since the predominant cell types transfected by naked m/Luc at the ear-pinnae would be MHC-II negative such as muscle cells, fibroblasts and keratinocytes [7], we speculate several reasons for this observation: First, the majority of cells that take up and express mRNA could have been muscle cells, which are well known to be more efficiently transfected by naked nucleic acid. Second, uptake mechanisms for n/RNA and p/mRNA are different with the former significantly more efficient than the latter. Indeed naked mRNA uptake is facilitated by nucleic acid specific receptors [7], while nanoparticles uptake may have to depend on other non-specific endocytic mechanisms, which may be directed into various degradative pathways. In this study we include an additional SubQ site at the base-of-tail, which not only is a favorable site for lymphatic drainage (5% Evans Blue injected subcutaneously at base-of-tail labels the inguinal lymph node within 30min [23]), but also serves as an additional control to ear pinna site. We find consistent trends of higher transfection efficiency by n/mLuc over p/mLuc at both ear pinna and base-of-tail sites, indicating that SubQ may not be an ideal vaccination site for p/mLuc.

An interesting finding from our study is that in vivo luciferase levels decay exponentially in a consistent manner regardless of format or site of administration. Hence apparent in vivo half-lives of luciferase protein expressed from mRNA, at given doses used in this study, can be computed. We noted earlier that apparent half-lives found between BOT and EP sites are different for subcutaneous n/mLuc transfection. This can be attributed to the difference in cell type subdistribution at both sites as the BOT site is significantly more muscular than ear pinnae.

Our reasoning is also supported by Fig.4, where transfection enhancement by RL is much smaller at BOT (Fig.4B) compared to that at EP (Fig.4A). Cells found in the former respond more favorably to naked mRNA, reducing the need of RL for enhancement. Due to a different cellular makeup, intracellular stability of mLuc and/or luciferase protein consequently varies between both sites.

Luciferase expression can be further extrapolated towards background levels to predict duration of gene expression. For SubQ-EP, detectable expression of both n/mLuc and p/mLuc can be extrapolated to 2-3 days, which is consistent with n/mLuc data from Probst et al (3 days) [7]. As one of the attractions of mRNA delivery is its transient nature, our data further support the idea that mRNA gene expression can be predictable and potentially controllable. This will help accelerate the translation of mRNA therapeutics into clinics.

Conclusion
In vitro and *in vivo* transfection efficiency and transgene expression kinetics of mRNA in naked and nanoparticle format are evaluated. We show that primary DCs can be efficiently transfected with mRNA nanoparticles with gene expression decaying in a biphasic manner. mRNA nanoparticles are also efficient *in vivo* when administered intranasally and intravenously, while naked mRNA dissolved in Ringer's Lactate is the most efficient at subcutaneous sites (ear pinna and base-of-tail). Gene expression at all sites decays in consistent exponential trends, which may render mRNA gene therapy not only safe but also predictable. This study shows that mRNA therapeutics adds to the armamentarium of biologics that can impact genetic medicine and warrants further research.

Acknowledgements

References Cited [1, 2, 4-12, 17, 20, 23-29][1, 2, 4-13, 18, 21, 24-29][1-13, 18, 21, 24-28]

1. D. Boczkowski, Nair S.K., Snyder D., and Gilboa E., Dendritic cells pulsed with RNA are potent antigen-presenting cells in vitro and in vivo. J Exp Med 1996 184(2) 465-472.

2. V.F. Van Tendeloo, Ponsaerts P., Lardon F., Nijs G., Lenjou M., Van Broeckhoven C., Van Bockstaele D.R., and Berneman Z.N., Highly efficient gene delivery by mRNA electroporation in human hematopoietic cells: superiority to lipofection and passive pulsing of mRNA and to electroporation of plasmid cDNA for tumor antigen loading of dendritic cells. Blood 2001 98(1) 49-56.

3. E.H. Aarntzen, Schreibelt G., Bol K., Lesterhuis W.J., Croockewit A.J., de Wilt J.H., van Rossum M.M., Blokx W.A., Jacobs J.F., Duiveman-de Boer T., Schuurhuis D.H., Mus R., Thielemans K., de Vries I.J., Figdor C.G., Punt C.J., and Adema G.J., Vaccination with mRNA-Electroporated Dendritic Cells Induces Robust Tumor Antigen-Specific CD4+ and CD8+ T Cells Responses in Stage III and IV Melanoma Patients. Clin Cancer Res 2012 18(19) 5460-5470.

4. S. Holtkamp, Kreiter S., Selmi A., Simon P., Koslowski M., Huber C., Tureci O., and Sahin U., Modification of antigen-encoding RNA increases stability, translational efficacy, and T-cell stimulatory capacity of dendritic cells. Blood 2006 108(13) 4009-4017.

5. A.N. Kuhn, Diken M., Kreiter S., Selmi A., Kowalska J., Jemielity J., Darzynkiewicz E., Huber C., Tureci O., and Sahin U., Phosphorothioate cap analogs increase stability and translational efficiency of RNA vaccines in immature dendritic cells and induce superior immune responses in vivo. Gene Ther 2010 17(8) 961-971.

6. K. Kariko, Muramatsu H., Welsh F.A., Ludwig J., Kato H., Akira S., and Weissman D., Incorporation of pseudouridine into mRNA yields superior nonimmunogenic vector with increased translational capacity and biological stability. Mol Ther 2008 16(11) 1833-1840.

7. J. Probst, Weide B., Scheel B., Pichler B.J., Hoerr I., Rammensee H.G., and Pascolo S., Spontaneous cellular uptake of exogenous messenger RNA in vivo is nucleic acid-specific, saturable and ion dependent. Gene Ther 2007 14(15) 1175-1180.

8. H. Wurtele, Little K.C., and Chartrand P., Illegitimate DNA integration in mammalian cells. Gene Ther 2003 10(21) 1791-1799.

9. S. Van Lint, Goyvaerts C., Maenhout S., Goethals L., Disy A., Benteyn D., Pen J., Bonehill A., Heirman C., Breckpot K., and Thielemans K., Preclinical evaluation of TriMix and antigen mRNA-based antitumor therapy. Cancer Res 2012 72(7) 1661-1671.

10. X. Su, Fricke J., Kavanagh D.G., and Irvine D.J., In vitro and in vivo mRNA delivery using lipid-enveloped pH-responsive polymer nanoparticles. Mol Pharm 2011 8(3) 774-787.

11. F. Perche, Benvegnu T., Berchel M., Lebegue L., Pichon C., Jaffres P.A., and Midoux P., Enhancement of dendritic cells transfection in vivo and of vaccination against B16F10 melanoma with mannosylated histidylated lipopolyplexes loaded with tumor antigen messenger RNA. Nanomedicine 2011 7(4) 445-453.

12. S.K. Nair, Heiser A., Boczkowski D., Majumdar A., Naoe M., Lebkowski J.S., Vieweg J., and Gilboa E., Induction of cytotoxic T cell responses and tumor immunity against unrelated tumors using telomerase reverse transcriptase RNA transfected dendritic cells. Nat Med 2000 6(9) 1011-1017.

13. S. Zou, Scarfo K., Nantz M.H., and Hecker J.G., Lipid-mediated delivery of RNA is more efficient than delivery of DNA in non-dividing cells. Int J Pharm 2010 389(1-2) 232-243.

14. C. Lin, Zhong Z., Lok M.C., Jiang X., Hennink W.E., Feijen J., and Engbersen J.F., Novel bioreducible poly(amido amine)s for highly efficient gene delivery. Bioconjug Chem 2007 18(1) 138-145.

15. C. Cheng, Convertine A.J., Stayton P.S., and Bryers J.D., Multifunctional triblock copolymers for intracellular messenger RNA delivery. Biomaterials 2012 33(28) 6868-6876.

16. L. Torrieri-Dramard, Lambrecht B., Ferreira H.L., Van den Berg T., Klatzmann D., and Bellier B., Intranasal DNA vaccination induces potent mucosal and systemic immune responses and cross-protective immunity against influenza viruses. Mol Ther 2011 19(3) 602-611.

17. F. Leuschner, Dutta P., Gorbatov R., Novobrantseva T.I., Donahoe J.S., Courties G., Lee K.M., Kim J.I., Markmann J.F., Marinelli B., Panizzi P., Lee W.W., Iwamoto Y., Milstein S., Epstein-Barash H., Cantley W., Wong J., Cortez-Retamozo V., Newton A., Love K., Libby P., Pittet M.J., Swirski F.K., Koteliansky V., Langer R., Weissleder R., Anderson D.G., and Nahrendorf M., Therapeutic siRNA silencing in inflammatory monocytes in mice. Nat Biotechnol 2011 29(11) 1005-1010.

18. B. Yu, Zhu J., Xue W., Wu Y., Huang X., Lee L.J., and Lee R.J., Microfluidic assembly of lipid-based oligonucleotide nanoparticles. Anticancer Res 2011 31(3) 771-776.

19. L.H. Hung, Teh S.Y., Jester J., and Lee A.P., PLGA micro/nanosphere synthesis by droplet microfluidic solvent evaporation and extraction approaches. Lab Chip 2010 10(14) 1820-1825.

20. Y.P. Ho, Grigsby C.L., Zhao F., and Leong K.W., Tuning physical properties of nanocomplexes through microfluidics-assisted confinement. Nano Lett 2011 11(5) 2178-2182.

21. J. Wang, Zhang P.C., Mao H.Q., and Leong K.W., Enhanced gene expression in mouse muscle by sustained release of plasmid DNA using PPE-EA as a carrier. Gene Ther 2002 9(18) 1254-1261.

22. J. Wang, Zhang P.C., Lu H.F., Ma N., Wang S., Mao H.Q., and Leong K.W., New polyphosphoramidate with a spermidine side chain as a gene carrier. Journal of Controlled Release 2002 83(1) 157-168.

23. M.I. Harrell, Iritani B.M., and Ruddell A., Lymph node mapping in the mouse. J Immunol Methods 2008 332(1-2) 170-174.

24. L. Warren, Manos P.D., Ahfeldt T., Loh Y.H., Li H., Lau F., Ebina W., Mandal P.K., Smith Z.D., Meissner A., Daley G.Q., Brack A.S., Collins J.J., Cowan C., Schlaeger T.M., and Rossi D.J., Highly efficient reprogramming to pluripotency and directed differentiation of human cells with synthetic modified mRNA. Cell Stem Cell 2010 7(5) 618-630.

25. J.C. Lorenzi, Trombone A.P., Rocha C.D., Almeida L.P., Lousada R.L., Malardo T., Fontoura I.C., Rossetti R.A., Gembre A.F., Silva A.M., Silva C.L., and Coelho-Castelo A.A., Intranasal vaccination with messenger RNA as a new approach in gene therapy: use against tuberculosis. BMC Biotechnol 2010 10 77.

26.   K. Kariko, Muramatsu H., Keller J.M., and Weissman D., Increased erythropoiesis in mice injected with submicrogram quantities of pseudouridine-containing mRNA encoding erythropoietin. Mol Ther 2012 20(5) 948-953.

27.   P. Hersey, Menzies S.W., Halliday G.M., Nguyen T., Farrelly M.L., DeSilva C., and Lett M., Phase I/II study of treatment with dendritic cell vaccines in patients with disseminated melanoma. Cancer Immunol Immunother 2004 53(2) 125-134.

28.   M. Diken, Kreiter S., Selmi A., Britten C.M., Huber C., Tureci O., and Sahin U., Selective uptake of naked vaccine RNA by dendritic cells is driven by macropinocytosis and abrogated upon DC maturation. Gene Ther 2011 18(7) 702-708.

29.   F. Blanco, Kalsi J., and Isenberg D.A., Analysis of antibodies to RNA in patients with systemic lupus erythematosus and other autoimmune rheumatic diseases. Clin Exp Immunol 1991 86(1) 66-70.
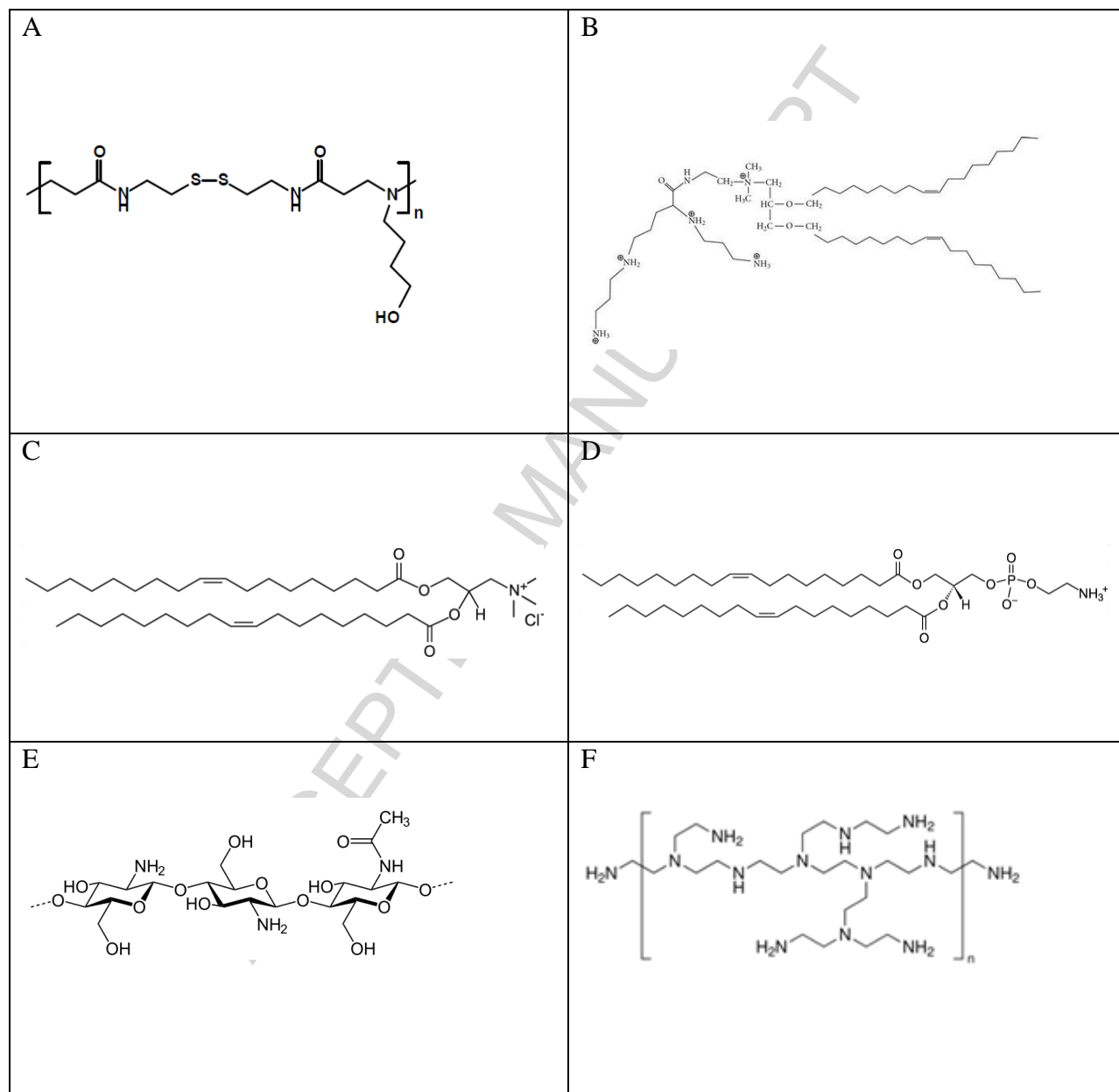
Supplementary Figures.
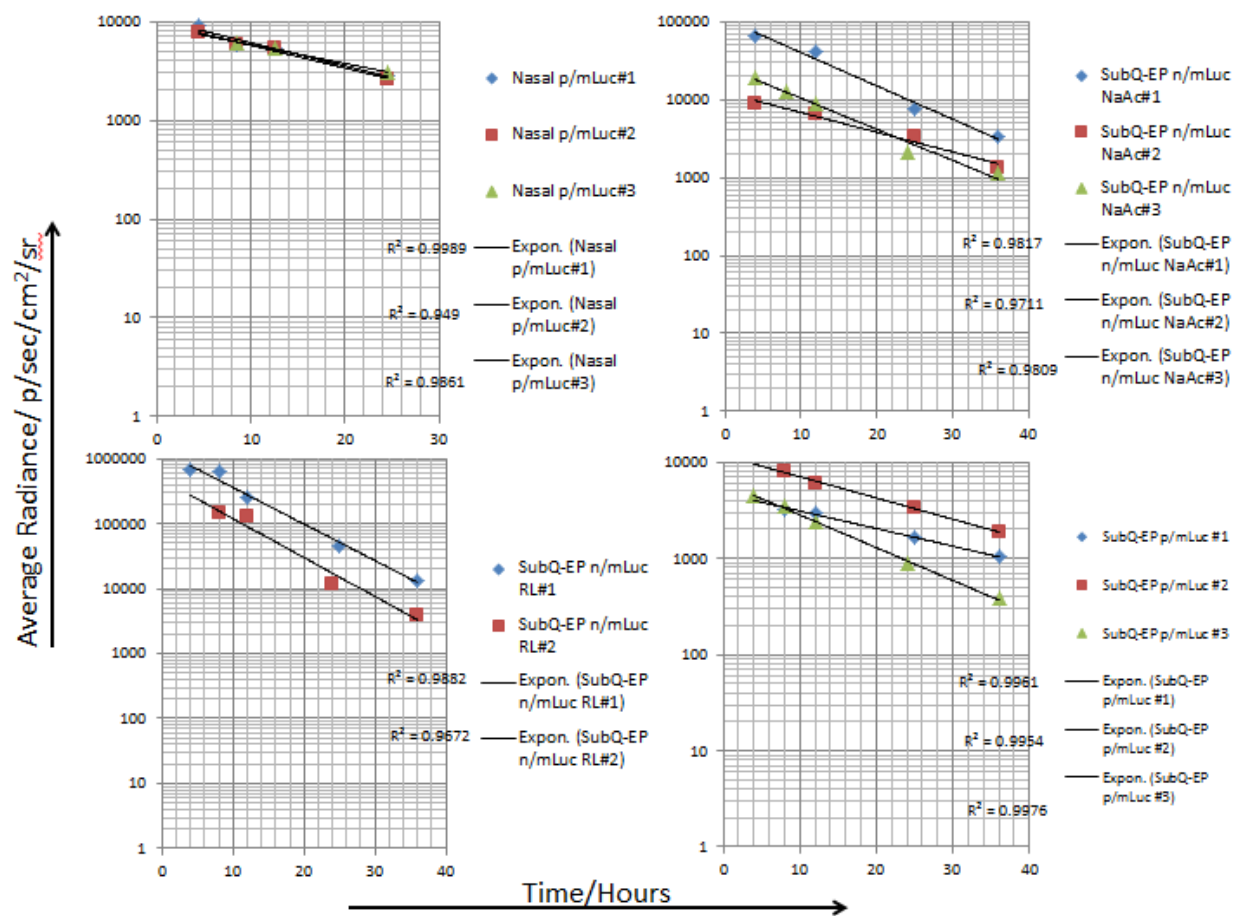
Supplementary S 1 .Regression analysis of additional transgene expression kinetics experiment performed in this study.

|	4h-n/mLuc	8h n/mLuc	12h n/mLuc	p/mOVA (4-36h)	NTC+ (4-36h)
4h-p/mLuc	**			**	
8h-p/mLuc		*		***	
12h-p/mLuc			**	***	
4h-n/mLuc (RL)	**				***
8h n/mLuc (RL)		ns			*
12h n/mLuc (RL			*		**
NTC+ (4-36h)	***	***	***	***	

Supplementary S 2. Comprehensive statistical analysis of data presented in Fig. 4A.

Supplementary S 3. Gene carriers preliminarily screened for mRNA nanoparticle transfection on JAWS II cell line. A. CBA-ABOL, B. Lipofectamine, C. DOTAP (1,2-dioleoyl-3-trimethylammonium-propane), D. DOPE (1,2-dioleoyl-*sn*-glycero-3-phosphoethanolamine), E. Chitosan, F. PEI (25kda)
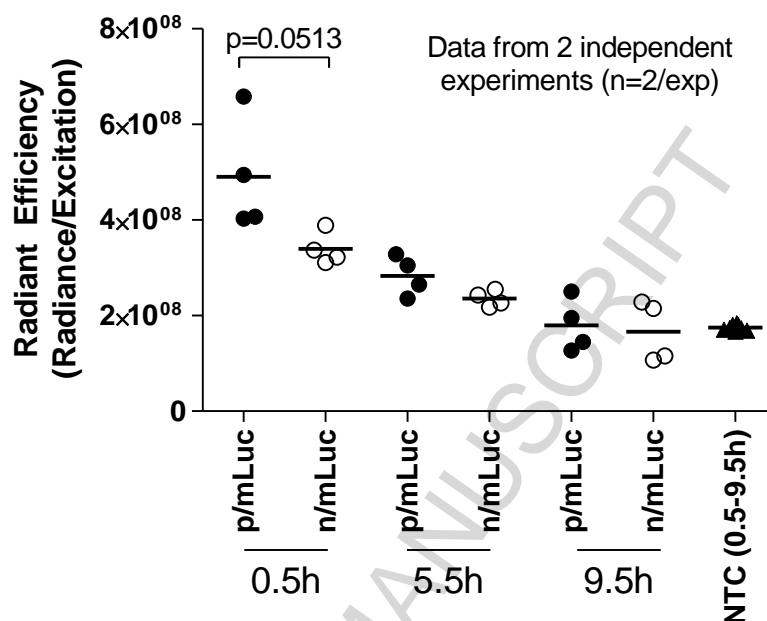
Supplementary S 4. 4 μg of Cy-5 labeled mLuc was administered intranasally into Balb/c mice. Cy-5 fluorescence was monitored at indicated time points using IVIS Kinetics Imaging System. Results from 2 independent experiments (n=2/group) were normalized to respective non-transfected controls (NTC) and plotted on the same graph.
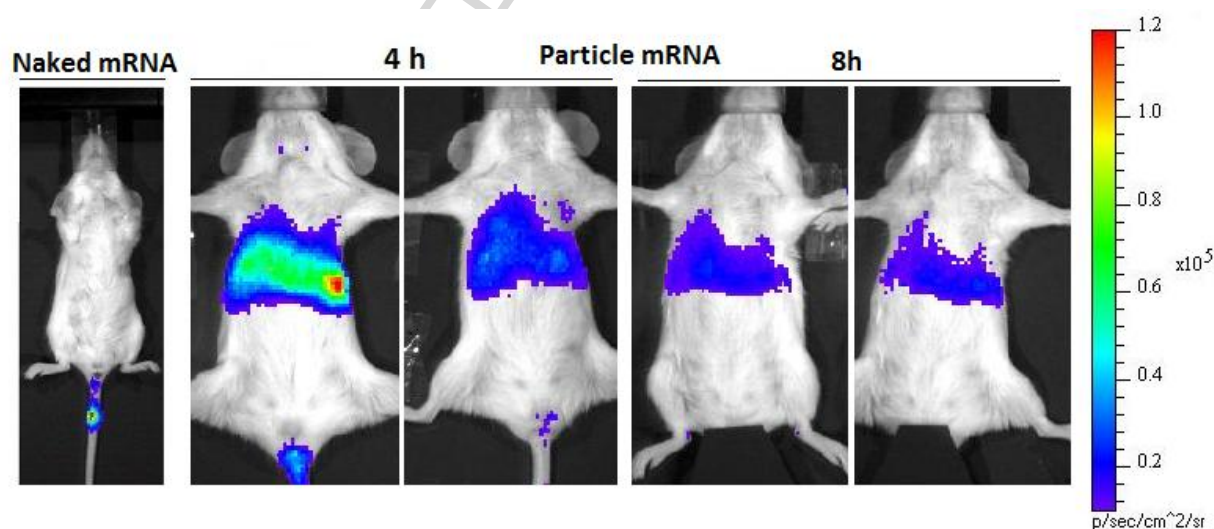
Supplementary S 5. Bioluminescence signal in BALB/c mice intravenously administered with 26 μg of partially aggregated p/mLuc at 4 and 8-hour post injection.
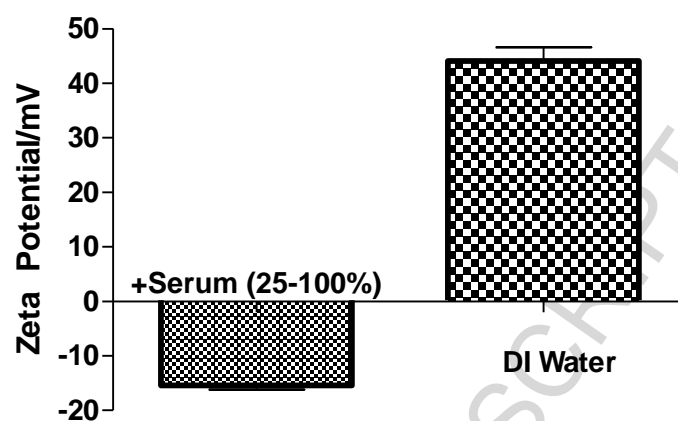
Supplementary S 6. Zeta potential of mRNA nanoparticles applied in this study.
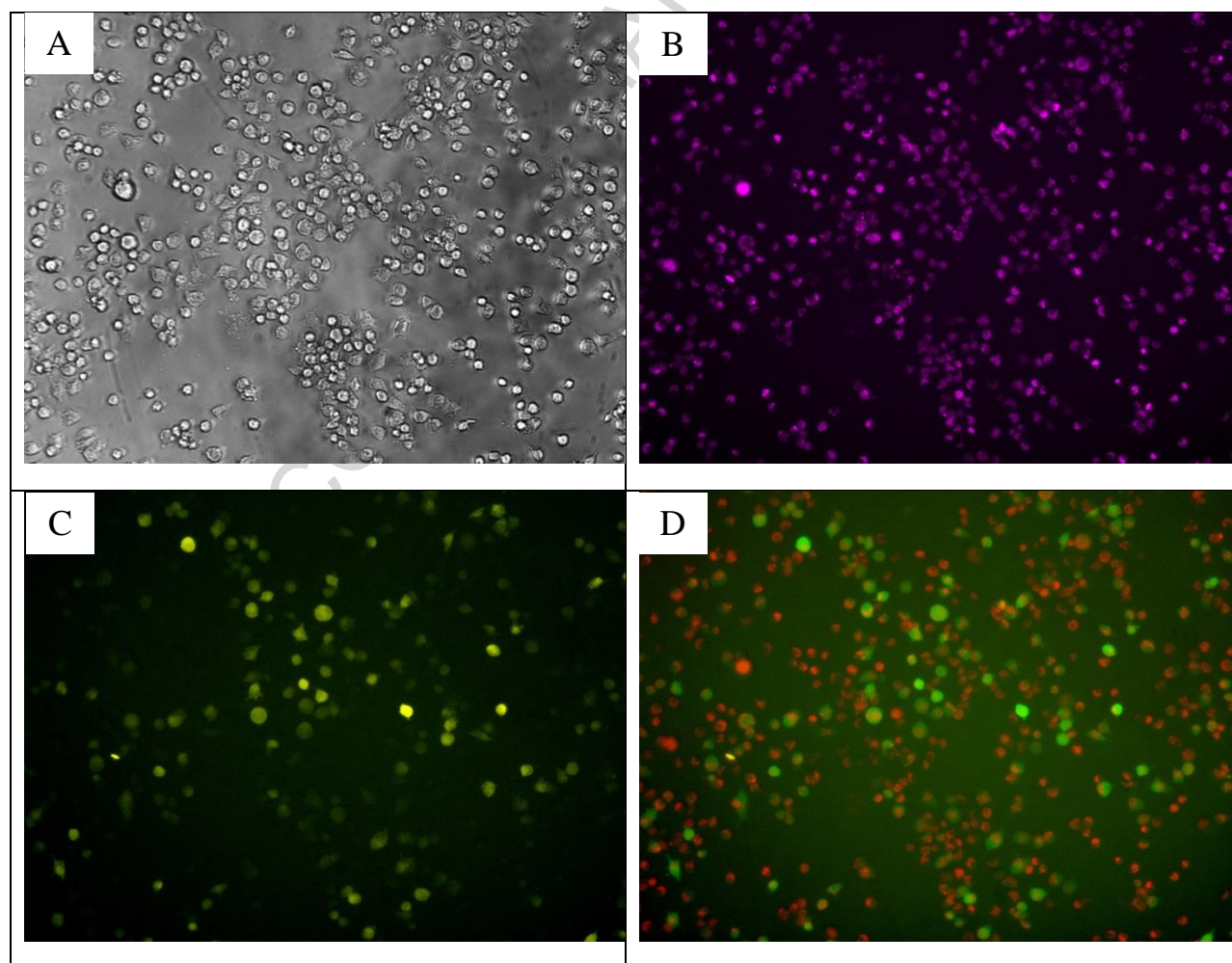
Supplementary S 7. Fluorescence microscope images of JAWS II cell transfected with nanoparticles co-encapsulating GFP and Cy5 labeled GFP mRNA. A. Bright field. B. Cy5-labeled mGFP. C. GFP expression. D. GFP/Cy5 merge.